RBMO

ELSEVIER

ARTICLE

Metformin reverses infertility in a mouse model of endometriosis: unveiling disease pathways and implications for future clinical approaches

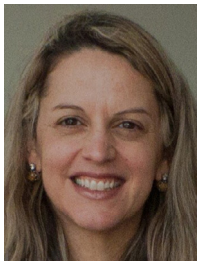

BIOGRAPHY

Delminda Neves, PhD, is Associated Professor in the Department of Biomedicine Unit of Experimental Biology of the Faculty of Medicine, and Senior Researcher in the group Ageing & Stress of IBMC/i3S at the University of Porto, Portugal.

A. Catarina Neto[1,2], Maria Botelho[1,2], Adriana R. Rodrigues[1,2,3], Sofia Lamas[2], Beatriz Araújo[4], J. Tiago Guimarães[5,6,7], Alexandra M. Gouveia[1,2], Henrique Almeida[1,2,8], Delminda Neves[1,2,*]

KEY MESSAGE

Treatment with metformin in a subtherapeutic dose enhances fertility rates in a mouse model of endometriosis by protecting against oxidative stress during pregnancy. Additionally, metformin reduces fibrosis, a process associated with the disease, particularly within endometriosis lesions.

ABSTRACT

Research question: Does metformin reverse endometriosis-associated infertility?

Design: Endometriosis was induced by transplanting uterus fragments from B6CBAF1 mice into recipients of the same strain. The mice were divided into groups: endometriosis (End, $n = 24$), sham-operated (Sham, $n = 12$), endometriosis with metformin (0.5mg/ml) orally administered for 3 months (EndMet, $n = 21$) and sham-operated metformin-treated (ShamMet, $n = 16$). Implant growth was monitored using ultrasonography. Fibrosis was computer-assisted quantified in Masson's trichrome-stained sections of eutopic (EuEnd) and ectopic (EcEnd) endometrium. PCNA, CYP17a1, F4/80 and galectin-3 were analysed by immunofluorescence and western blotting, and NFkB, GPX-1 and HO-1 only by western blotting. Statistical significance was set at $P < 0.05$.

Results: The endometriosis model was successfully established. The End groups showed lower fertility rates than sham-operated mice ($P = 0.0034$), whereas metformin treatment increased the number of fetuses per pregnant mouse ($P = 0.0295$), restoring fertility to control levels; it also slowed implant growth and vascularization. Metformin also restored PCNA expression and fibrosis levels to those of non-treated EuSham mice. PCNA expression decreased in pregnant mice ($P < 0.0178$). Metformin diminished CYP17a1 expression in EcEnd versus EuEnd non-treated tissues and conversely up-regulated F4/80 in EuEnd tissue ($P < 0.0170$), and galectin-3, NFkB and the antioxidant enzymes HO-1 and GPX-1 in EcEnd tissue ($P < 0.0293$), in non-mated mice.

[1] Department of Biomedicine Experimental Biology Unit, Faculty of Medicine of the University of Porto, Porto, Portugal.
[2] Instituto de Investigação e Inovação em Saúde (i3S), Porto, Portugal.
[3] Faculty of Nutrition and Food Sciences, University of Porto, Porto, Portugal.
[4] Serviço de Patologia Clínica da ULS de Braga, Braga, Portugal.
[5] Department of Biomedicine Biochemistry Unit, Faculty of Medicine, University of Porto, Porto, Portugal.
[6] Clinical Pathology, São João University Hospital Center, Porto, Portugal.
[7] EPIUnit, Institute of Public Health, University of Porto, Porto, Portugal.
[8] Obstetrics and Gynaecology, Hospital-CUF Porto, Porto, Portugal.

*Corresponding author. E-mail address: delmagal@med.up.pt (D. Neves). https://doi.org/10.1016/j.rbmo.2024.104474 1472-6483/
Declaration: Declaration: The authors report no financial or commercial conflicts of interest.

KEYWORDS
Endometriosis
Fertility
Inflammation
Metformin
Oxidative Stress
Reproductive health

Conclusions: These results indicate that application of metformin can alleviate oxidative stress and mitigate fibrosis in endometriosis lesions in a murine model of endometriosis, which highlights metformin's potential as a pharmacological intervention for improving infertility in endometriosis.

INTRODUCTION

Infertility, defined as the absence of conception after 1 year of unprotected and regular intercourse, is a public health concern, driving a rising demand for assisted reproductive technology (ART) (*Inhorn and Patrizio, 2015*). One of the most prevalent worldwide causes of infertility in the female partner is endometriosis, affecting up to 40% of women facing infertility (*Cohen et al., 2015*; *Evans and Decherney, 2017*). Endometriosis is a gynaecological condition with systemic impact, marked by an oestrogen-dependent aberrant growth of vascularized endometrial-like tissue outside the uterus, predominantly within the pelvic region (*Alderman et al., 2017*; *Taylor et al., 2021*). This disorder results primarily in pelvic pain, the most common symptom in endometriosis patients, and, in the advanced stages, pelvic organ distortion and infertility.

The pathophysiology of endometriosis, in particular the associated infertility, is far from being completely elucidated, but it is known that disease progression encompasses an inflammatory reaction, cellular proliferation, migration, invasion and angiogenesis (*Samimi et al., 2019*). Substantial evidence indicates that oxidative stress incites inflammation, through either an escalated production of reactive oxygen species or a decrease in antioxidant defences (*Clower et al., 2022*). The continuing inflammatory stimulus underlies the loss of function and the fibrosis of endometrial tissue that is closely associated with endometriosis (*Viganò et al., 2020*).

Endometriosis patients often require ART treatments, primarily due to the inadequacy of the hormone-based treatments currently used to control the disease (*Coccia et al., 2022*). In addition, these treatments must be interrupted before and during pregnancy, which frequently leads to symptom aggravation (*Skorupskaite and Bhandari, 2021*). In this context, there is an unmet need for new pharmacological strategies to control endometriosis both before conception and during pregnancy.

In rodents, endometriosis is not a natural disorder. However, a surgically induced model of endometriosis in rats is associated with anomalies of the hypothalamic–pituitary–ovarian axis, ovarian follicle development, oocyte quality and embryo development and implantation, as well as ovulatory and hormone/receptor dysfunction and an inflammatory milieu in the peritoneal cavity (*Sharpe-Timms et al., 2020*). In addition, familial aspects of endometriosis and transgenerational subfertility in both female and male offspring over three generations have been demonstrated in a rat model of endometriosis (*Sharpe-Timms et al., 2020*; *Stilley et al., 2009*).

In line with this, induced peritoneal endometriosis in a mouse model has been shown to be associated with a decrease in oocyte quality and embryo number. In these animals, fertility is impacted by the volume of tissue implanted as endometriotic lesions, and thus the induced disease can be modulated by various therapeutic approaches (*Cohen et al., 2015*; *Greaves et al., 2014*; *Park et al., 2022*; *Pelch et al., 2012*; *Rosa-E-Silva et al., 2019*). Conversely, an earlier study reported that although the pregnancy rate was decreased in a mouse model of endometriosis, no significant differences in resorption rate, litter size and pup weight were noted between groups (*Bilotas et al., 2015*). These differences may be attributed to differences in the models or murine strains used. In sum, despite the differences observed between experimental rodent models of endometriosis, they provide valuable insights into the pathophysiology of endometriosis-associated infertility and enable the assessment of novel pharmacological interventions.

One of the putative drugs for controlling endometriosis is metformin, a widely employed medication for type 2 diabetes. Interestingly, owing to its antioxidant properties, it instigates the regression of endometrial implants in a rat model of endometriosis (*Viollet et al., 2012*; *Yilmaz et al., 2010*). In addition, metformin curtails cell proliferation, suppresses the secretion of pro-inflammatory cytokines and lowers oestrogen production in cultured human endometrioma-derived stromal cells, underscoring its anti-inflammatory attributes (*Takemura et al., 2007*).

Moreover, metformin has been safely and effectively used in the management of gestational diabetes, demonstrating no adverse effects on women or embryos (*Ainuddin et al., 2015*).

Despite these encouraging effects on controlling the progression of endometriosis, the particular impact of metformin on fertility in endometriosis has not, to the best of the current authors' knowledge, been elucidated. Thus, the goal of this study was to assess whether metformin would be effective in stopping the progression of endometriosis features and improve the associated infertility. In addition, it aimed to explore the likely mechanisms underlying this benefit.

MATERIAL AND METHODS

Mouse model of endometriosis

All experiments were approved by the Institute for Research and Innovation in Health (i3S) Animal Ethical Committee and the Portuguese Competent Authority (Direcção-Geral de Alimentação e Veterinária, internal reference 2018/27). All the procedures employed in this study adhere to European Community Council directive 2010/63/EU and to the ARRIVE (Animal Research: Reporting of *In Vivo* Experiments) 2.0 guidelines.

Seventy-three 8-week-old B6CBAF1 female mice descended from female CBA/J mice mated with male C57BL/6J mice (Charles River Laboratories, France) were employed in the experiments, which were carried out at i3S (Porto, Portugal). The mice had free access to food (2014S, Envigo, UK) and water. They were housed five per cage in a room with controlled temperature and humidity (21°C and 50%, respectively), and under a 12/12 h light/dark cycle. All the cages had paper for nesting and cardboard rolls. The oestrous cycle stage of the mice was analysed in each animal before the experiments by vaginal inspection and cytological smear, confirming that all the animals were at a similar stage of the oestrous cycle.

Endometriosis was surgically induced in 45 randomly selected recipient mice by heterologous transplantation of endometrial tissue fragments harvested

from B6CBAF1 mice donors, according to the method described by Cohen and colleagues (*Cohen et al., 2015*). Briefly, 8-week-old donor mice were subjected to general anaesthesia with isoflurane (B. Braun, Germany) and euthanized by cervical dislocation. Both uterine horns were removed and placed in warm Ringer's lactate solution in a Petri dish. The uterine horns were then longitudinally opened with micro-scissors under a stereomicroscope (Olympus SZX10, Olympus Europa, Germany) and divided under micro-ruler guidance into tissue fragments measuring approximately 3 mm^3.

Subsequently, the recipient mice were anaesthetized using isoflurane, and buprenorphine (Bupaq, 0.08 mg/kg subcutaneously) was given as analgesia. After surgical preparation, a small incision was made into the ventral abdominal cavity, followed by a second incision in the peritoneum. One tissue fragment was attached with a 7-0 non-absorbable suture to the right peritoneal wall and an additional fragment to the left peritoneal wall of each recipient mouse, a previous study having demonstrated that the impact on fertility was equivalent whether two or four fragments were implanted in the uterine wall of recipient mice (*Rosa-E-Silva et al., 2019*). Finally, the peritoneum and the skin were closed with a 6-0 absorbable suture. Mice were treated with buprenorphine 0.1 mg per 100 g body weight administered subcutaneously every 12 h for 72 h. In addition, suture sites and pain signals of pain were checked daily. Sham-operated mice were used as control group ($n = 28$). In these animals the same procedures were performed but, instead of attaching a tissue fragment, a 7-0 non-absorbable suture was placed in the right and in the left abdominal wall.

For each mouse, an endometriosis-like phenotype was confirmed by ultrasound visualization of the implanted endometrial tissue (Micro Ultrasound Vevo 2100, VisualSonics, Canada). The evolution of the implant growth was monitored for 3 months at three timepoints by measuring the area of the implant (pixel^2) using AxioVision 4.8 software (Carl Zeiss, Germany) after determining the height and width of the area, including its brim on a two-dimensional image of the implant. The first timepoint was 1 month after the surgery to induce endometriosis, and timepoints 2 and 3 were at 45 and 90 days after timepoint 1. The first image was considered to indicate timepoint 1 and the growth at the remaining timepoints was evaluated by calculating the ratio of the implant area at each timepoint relative to the area at timepoint 1.

The animals were divided into four groups: mice with surgically induced endometriosis (End, $n = 24$); sham-operated mice (Sham, $n = 12$); mice with endometriosis treated with metformin (EndMet, $n = 21$); and Sham-operated mice treated with metformin (ShamMet, $n = 16$). Metformin (Alfa Aesar Chemicals, USA) was administered orally (0.5 mg/ml diluted in drinking water) for 3 months starting at timepoint 1, and the average dose per mouse was further determined based on the volume of water ingested per day. Each bottle was weighed when it was placed in the animal cage and again at every 2-day change. Bottles were excluded from the calculations if there had been sporadic liquid spillage. The initial weight of the animals was registered on the day of surgery and the final weight just before euthanasia.

Twenty-four hours after the treatment had been completed, the mice in each group were randomly divided into two subgroups. One group was use to assess the fertility rate. The other was anaesthetized for blood collection, abdominal examination and collection of tissue samples; the volatile anaesthetic was maintained until euthanasia was confirmed. The vaginas of the mice were inspected and no differences were identified between the mice, either within the same group or between the different groups, confirming that they were at a similar stage of the oestrous cycle stage at euthanasia. During the abdominal examination, the anatomy of the reproductive system organs was verified by visual macroscopic inspection in every animal at the end-point (FIGURE 1A depicts the study design and exact number of animals per group).

The weight, width, height and length of the implants in each mouse were measured with callipers. One implant was immediately frozen on liquid nitrogen, and the other was placed in 10% buffered formaldehyde. In addition, both uterine horns and the site of the peritoneal wall where the implants/sutures had been placed were collected and divided into two portions. The frozen tissue fragments were stored at −80°C for posterior analysis, and the fixed fragments were embedded in paraffin.

Serum analysis

After blood had been collected from the left ventricle, the serum was separated by blood centrifugation at 300*g* for 15 min and preserved at −20°C for further biochemical analysis. Serum glucose concentrations were determined at the experimental end-point using a glucose analyser (OneTouch Ultra, LifeScan, USA). Serum total cholesterol and high-density lipoprotein cholesterol (HDL-C) concentrations were determined by enzymatic colorimetry using an Olympus AU5800 autoanalyser (Beckman Coulter, USA) using commercial kits (OSR6616 and OSR6687, respectively; Beckman Coulter) as per the manufacturer's instructions. Low-density lipoprotein cholesterol (LDL-C) concentrations were calculated using Friedewald's formula (LDL-C = total cholesterol − [HDL-C − 1/5 triglyceride] if the serum triglyceride concentration is 400 mg/dl or less).

Oestradiol concentrations were determined using electrochemiluminescence technology for immunoassay analysis in a Cobas E411 autoanalyser (Roche Diagnostics, USA) utilizing the commercial kit (03000070190, Roche Diagnostics).

Fertility rate assessment

The female mice used for fertility assessment were mated with healthy B6CBAF1 males aged 5 months — one male and two females per cage over 3 days. Mice were checked daily and mating was confirmed by the presence of a vaginal plug. On the 18th day after mating the animals were euthanized as described above. Animals that did not present a vaginal plug ($n = 4$) were excluded from the study, and animals showing a plug were confirmed to be pregnant. Fertility rates were assessed by evaluating the mean number of fetuses per pregnant mouse in each group. Reabsorptions were also quantified in every pregnant mouse.

Morphological analysis of the uterus and implants

Sections of paraffin-embedded uterine horn and ectopically implanted endometrial tissue (5 μm) were assembled on poly-L-lysine-coated slides. The sections were stained with haematoxylin and eosin (H&E) for morphological examination. Briefly, sections were dewaxed by incubating them twice (for 10 and 5 min) in xylol (Merck, Germany) and then hydrated by a series of 5 min incubations in aqueous ethanol solutions of decreasing

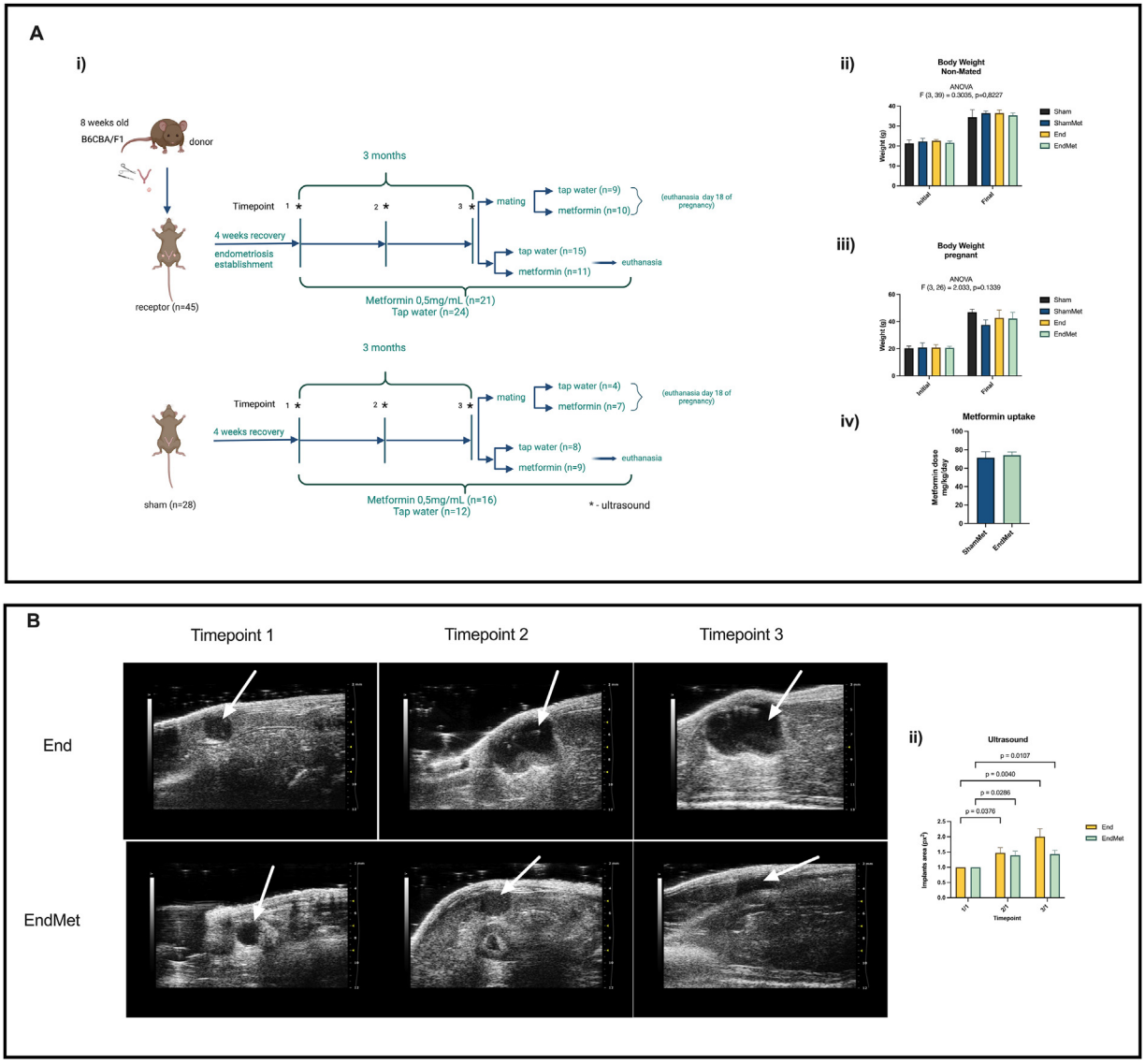

FIGURE 1 Metformin reduces the rate of endometriosis progression. (A) (i) Study design for the mouse model indicating the number used at each stage of the experiment: non-mated Sham (8); non-mated ShamMet (9); non-mated End (15); non-mated EndMet (11); pregnant Sham (4); pregnant ShamMet (7); pregnant End (9); and pregnant EndMet (10). Image created in BioRender. (ii, iii) Graphical depiction of the change in weight of the mice between the day of the surgery and the day of euthanasia in (ii) non-mated and (iii) pregnant mice. (iv) Assessment of the effective dose of metformin imbibed by the mice in the ShamMet and EndMet groups. (B) (i) Representative ultrasound images of implants in mice in the End and EndMet groups at the three timepoints; white arrows indicate the implants. (ii) Graphical analysis of implant growth rate versus time. Values are normalized to timepoint 1 (1 unit in px^2 was considered for relativization of the area). (C) (i) Representative images showing the non-absorbable sutures (black arrows) in Sham mice. (ii, iii) Endometriosis implants (yellow arrows) in End mice. The magnified inset in (ii) shows the vascularization of an implant (yellow arrow). (iv) Endometriosis implant in EndMet mice. The implants in the mice treated with metformin (yellow arrow) were of a clearer colour than those observed in the non-treated animals, which appeared red. (D) Serum analysis of (i) oestradiol, (ii) total cholesterol, (iii) high-density lipoprotein (HDL) cholesterol, (iv) low-density lipoprotein (LDL) cholesterol and (v) glucose in the experimental groups of non-mated and pregnant mice. Two-way analysis of variance (ANOVA) followed by post-hoc analyses using Tukey's multiple comparisons tests was employed for the statistical analysis, except for metformin uptake, which was analysed using a Student's t-test. Values are presented as mean ± SEM. Significant *P*-values shown in the figure, and all the *P*-values are shown in Supplementary Table 1. Sham, sham-operated mice; ShamMet, sham-operated mice treated with metformin; End, mice with endometriosis; EndMet, mice with endometriosis treated with metformin.

concentrations (100–50% v/v) and water. Afterwards, the sections were stained with Papanicolaou's solution 1a Harris' haematoxylin solution (Merck) for 2 min followed by washing for 15 min in tap water, and then stained with an alcoholic solution of eosin 0.5% (w/v) (Sigma-Aldrich, USA; when not specified, the reagents were acquired from Sigma-Aldrich) for 5 min. Finally, the tissue sections were dehydrated with solutions of increasing concentrations of ethanol in water followed by two passages in xylol. Sections were assembled with a coverslip and Entellan and air dried.

Masson's trichrome stain was applied to differentiate connective tissue, including

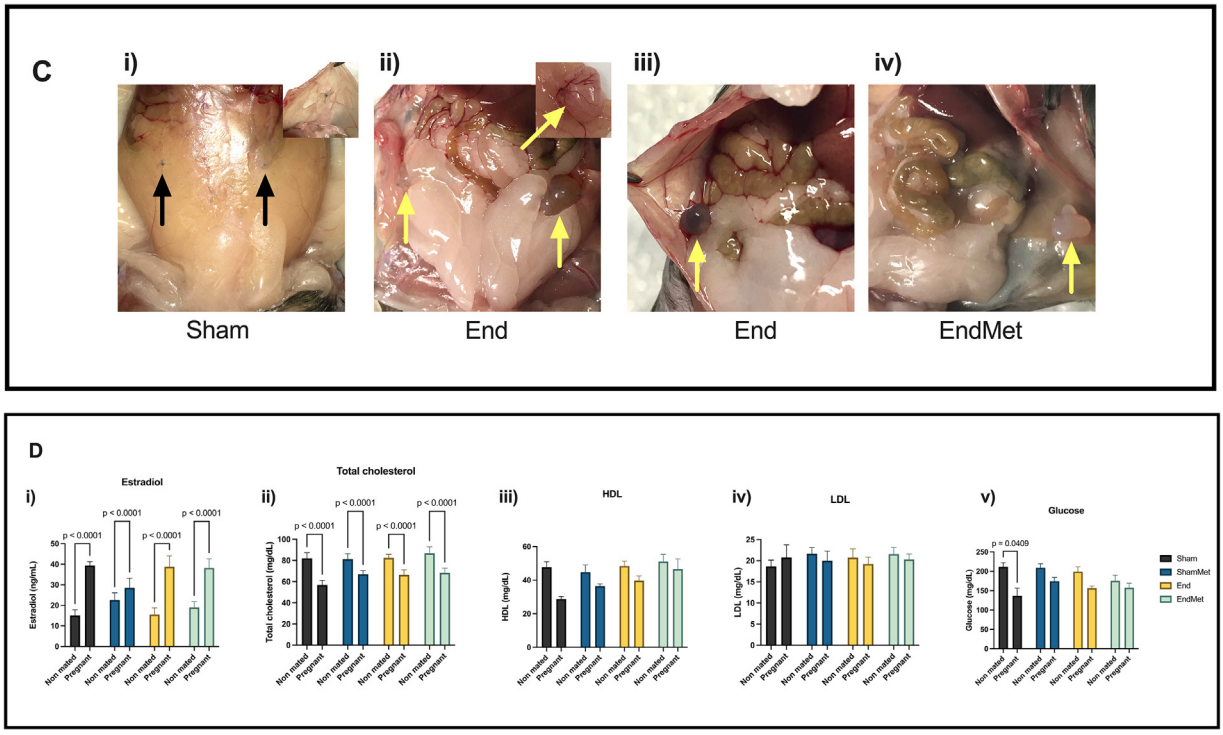

Figure 1 Continued.

collagen fibres and fibrin, from muscle and erythrocytes. The sections were dewaxed and hydrated as previously described and stained with Weigert's haematoxylin (0.5% w/v celestial, 5% w/v iron ammonium (III) dodecahydrate sulfate, VWR, USA) for 5 min and, immediately afterwards, 0.4% w/v Gill's haematoxylin solution for 5 min. Next, the sections were immersed in 1.3% w/v picric acid aqueous solution for 5 min and then washed in water, followed by staining with Biebrich scarlet–acid fuchsin solution (0.5% w/v Ponceau xylidine, 1% w/v acid fuchsin, Fisher Scientific, USA) for 15 min and incubated in 1% w/v molybdalophosphoric acid hydrate aqueous solution (VWR) for 5 min. After a washing step, the final staining was performed with 0.5% w/v light green (Bio-Optica, Italy) for 10 min. The sections were covered with 1% v/v acetic acid aqueous solution for 2 min and ultimately immersed in water, briefly passed through ethanol and dehydrated for 15 min in xylol before assembly with Entellan.

The sections were observed with 5 × (H&E) and 10 × (Masson's trichrome) magnification objectives lenses under a light Zeiss Axioskop 40 (Carl Zeiss) microscope, equipped with Zeiss Axiocam 208 Color camera (Carl Zeiss), and representative images were captured using Zen software (Carl Zeiss).

The area of fibrosis was quantified on images from Masson's trichrome-stained sections from the uterus and implants by computer-assisted morphometry. Eight fields on each tissue section (n = 6 mice per group) were analysed using Image-Pro Plus 6 software (Media Cybernetics, USA); the ratio of the green-coloured fibrotic area to the total tissue area, corresponding to the percentage of interstitial fibrosis, was calculated.

Immunofluorescence

Fluorescent immunolabelling was performed to identify proliferating cell nuclear antigen (PCNA) and cytochrome P450 (CYP)17a1, markers of cell proliferation and steroidogenesis, respectively. Double immunolabelling was performed to identify macrophage marker F4/80 and inflammation mediator and inflammatory cell marker galectin-3.

The uterine and ectopic tissue sections were dewaxed and hydrated as previously described. Sections were washed with phosphate-buffered saline (PBS) solution and permeabilized with 0.5% v/v Triton X-100 in PBS for 5 min, followed by two 5 min washes in PBS. After that, antigen recovery was undertaken with 1 mol/l HCl for 30 min at room temperature followed by neutralization with 2% w/v borax aqueous solution for 5 min. The sections were blocked with 2% w/v bovine serum albumin in PBS with 0.1% v/v Tween 20 (PBS-T) for 1 h at room temperature in a humid chamber, before overnight incubation at 4°C with rabbit anti-PCNA (0.27 μg/mL, AB_2636979, Cell Signaling, USA) or rabbit anti-CYP17a1 (0.3 μg/mL, AB_2800219, Cell Signaling) diluted in blocking solution.

The following day, the sections were washed thoroughly with PBS-T and incubated with anti-rabbit IgG secondary antibody conjugated with Alexa Fluor 488 (2 μg/ml, AB_2535792, Thermo Fisher, USA) diluted in PBS-T for 1 h at room temperature. Then, after washing, the nuclei were stained with 4′,6-diamidino-2-phenylindole (DAPI) and the sections assembled with 50% v/v glycerol/PBS. The double immunolabelling was performed as described above with slight differences in the method: the incubation with primary antibodies was undertaken using a mixture of rabbit anti-F4/80 (0.87 μg/ml, AB_2799771, Cell Signaling) and rat anti-galectin-3 (0.07 μg/ml, AB_627658, Santa Cruz Technology, USA) primary antibodies diluted in blocking solution, overnight at 4°C.

The next day the sections were incubated a mixture of secondary antibodies Alexa Fluor 568-conjugated anti-rabbit IgG

antibody (2 μg/ml; AB_2534017, Thermo Fisher) and biotinylated anti-rat IgG (0.14 μg/ml, AB_2315779, Jackson ImmunoResearch, USA) diluted in PBS-T for 1 h at room temperature; a fluorescent label was added to the biotinylated antibody through incubation with streptavidin Alexa Fluor 488 (2 μg/ml; Invitrogen, USA) diluted in PBS-T for 1 h. Sections were viewed with a 20 × magnification objective lens and images were recorded on an Apotome fluorescence microscope (AxioImager Z1, Carl Zeiss) equipped with a digital camera (AxioCam MRm, Carl Zeiss) and AxioVision 4.8 software (Carl Zeiss). Negative control experiments were performed with non-immune serum in place of the primary antibody and, additionally, with omission of the secondary antibodies (to exclude auto-fluorescence).

Western blotting

Total protein in samples of eutopic and ectopic endometrial tissue was quantified by the Bradford colorimetric method, after homogenization of tissues in lysis buffer at pH 7.6 (50 mmol/l Tris, 10 mmol/l NaCl, 5 mmol/l EDTA, 2 mmol/l β-glycerophosphate, 0.25% v/v Triton X-100) supplemented with inhibitors of proteases (0.5% v/v) and phosphatases (0.4% v/v) (Sigma-Aldrich). Then, 15 μg of total protein/sample was loaded on a discontinuous buffer electrophoresis system (Bio-Rad Laboratories, USA) using 12% sodium dodecylsulfate-polyacrylamide resolution gel electrophoresis to carry out electrophoretic separation. A constant electric current of 25 mA per gel was applied for approximately 1 h at room temperature.

After electrophoretic separation, the proteins were transferred to a 0.45 μm pore nitrocellulose membrane (Bio-Rad Laboratories), applying a potential difference of 30 V for 90 min. After staining with Ponceau S for 2 min the image of the separated protein bands on the membranes was captured and saved in a Chemidoc XRS (Bio-Rad Laboratories) for further normalization of the studied proteins. The membranes were then incubated with warm blocking solution (5% w/v non-fat powdered milk [Molico, Nestlé, Portugal] diluted in Tris-buffered saline with 0.1% v/v Tween-20 [TBS−T]) for 1 h at room temperature. The membranes were incubated with antibodies for at least two overnight sessions at 4°C with stirring; the antibodies were primary rabbit antibodies (Cell Signaling when the manufacturer is not indicated) diluted in blocking solution, anti-PCNA (0.134 μg/ml), anti-CYP17a1 (0.06 μg/ml), anti-F4/80 (0.435 μg/ml), anti-nuclear factor kappa B (NFκB; 0.42 μg/ml, AB_10859369), anti-heme oxygenase (HO-1; 0.13 μg/ml, AB_2118685, ProteinTech, USA), anti-glutathione peroxidase (GPX-1; 0.8 μg/ml, AB_2112120, Abcam) and rat antibody anti-galectin-3 (0.02 μg/ml).

The membranes were then washed with TBS-T solution and incubated with the appropriate secondary anti-rabbit antibody conjugated with horseradish peroxidase (AB_10015282, Jackson ImmunoResearch) for 1 h at room temperature with stirring; secondary anti-rat antibody conjugated with horseradish peroxidase (AB_1125219 Santa-Cruz Biotechnology) was used to detect galectin-3. Immunoreaction of each membrane was performed by applying a chemiluminescent substrate for peroxidase (Clarity Western ECL Substrates, Bio-Rad Laboratories) for 5 min, followed by signal detection using the Chemidoc XRS equipment.

To semi-quantify the immunolabelled bands, the intensity of the band, assessed by densitometry and with Image Lab® software (Bio-Rad Laboratories), was divided by the total staining of the proteins in the corresponding lane, stained with Ponceau S. To minimize the variations in exposure times between the membranes, the average intensity value of the uterine samples from the sham group on each membrane served as an internal control. In the experiments that compared only ectopic endometrial tissue samples harvested from non-mated and pregnant mice, the internal control in the membranes was the average value obtained for the samples from the non-mated End group. Each analysis involved a minimum of six distinct samples (mice) per group, and for each protein analysis every sample was quantified in at least two different gels, with the results averaged per sample.

Statistical analysis

Statistical analysis, including an assessment of data distribution normality, was undertaken using Prism version 9.5 (GraphPad Software, USA).

All analyses were performed after verifying normal distribution using the Shapiro−Wilk test. The Student's t-test was performed to analyse metformin uptake. One-way analysis of variance (ANOVA) was applied to evaluate pregnancy rates. Regular two-way ANOVA was applied to evaluate the effect of the combined factors: endometriosis and metformin, or pregnancy and metformin. In addition, post-hoc analyses were performed using Tukey's multiple comparisons tests.

The results are presented as mean ± standard error of the mean (SEM), and a P-value <0.05 was considered statistically significant.

RESULTS

Metformin reduces the rate of endometriosis progression

The establishment of the endometriosis mouse model was carried out as depicted in FIGURE 1Ai and proved to be successful because a growth of ectopic uterus implants was noted in all the mouse than had been operated on. A high rate of mouse survival was verified as only one death occurred during surgery and none in the follow-up. As metformin could be considered a mimetic of energy restriction, the body weight of the animals was assessed at the final end-point, but no differences were found between groups within the same pregnancy condition (non-mated or pregnant mice) (FIGURE 1Aii, iii). Based on the volume of liquid ingested, the effective dose of administered metformin was clinically similar for the ShamMet (71.3 mg/kg per day) and EndMet (74.15 mg/kg per day) groups (FIGURE 1Aiv).

The implant growth in the End and EndMet groups was visualized using ultrasound (FIGURE 1Bi). The End group exhibited a statistically significant growth of the implant area (pixel^2) at timepoints 2 and 3 relative to timepoint 1. However, the growth from timepoint 2 (1.47 times the area measured at timepoint 1) to timepoint 3 (2.00 times the area measured at timepoint 1) did not reach statistical significance (P = 0,1123). The EndMet group exhibited implant growth at timepoints 2 and 3 relative to timepoint 1, but between timepoints 2 and 3 the area only changed from 1.39 to 1.43 times the initially measured area (timepoint 1) (P = 0.8396; FIGURE 1Bii).

At the final end-point, reddish vascularized implants resembling cysts that adhered to several abdominal organs were identified in the mice from the End

group, providing evidence for the macroscopic similarities between the endometriotic implants observed in this animal model and those found in endometriosis patients. The implants in the EndMet group were visually a clearer colour than those in the End group (FIGURE 1Cii–iv). The stitches were clearly observed in the Sham group, but inflammatory signs were absent (FIGURE 1Ci).

No significant differences in the concentrations of oestradiol, total cholesterol, HDL-C, LDL-C and glucose in mouse serum were observed between the four treatment groups for either the non-mated or the pregnant mice (FIGURE 1D, Supplementary Table 1). However, when the non-mated and pregnant states were compared within the same group, a significant increase in oestradiol concentration and a concomitant decrease in total cholesterol concentrations were observed in the pregnant mice for all treatment conditions (all $P < 0.0001$; FIGURE 1Di, ii). In addition, a decrease in blood glucose concentrations was observed in the pregnant Sham mice compared with their non-mated Sham counterparts ($P = 0.0409$); however, this variation was not evident in either the End groups or the mice treated with metformin. It should also be noted that the animals were not fasting at the time of euthanasia, which augmented the variability of blood glucose concentrations.

Endometriosis increases fibrosis of endometrial tissue

Morphological similarities between eutopic and ectopic endometrial tissue were confirmed by H&E staining. It was possible to identify epithelial and stromal cells, as well as glands, in both tissues and in all the experimental groups,. Microscopic analysis confirmed the ability of implants to graft to the peritoneum (FIGURE 2i).

Observation of sections stained with Masson's trichrome indicated a noticeable increase in stromal fibrosis in the non-mated, non-treated animals with endometriosis compared with both Sham groups, in both eutopic tissues (non-treated EuEnd versus non-treated EuSham, $P = 0.0186$; and versus EuShamMet, $P = 0.0008$) and ectopic tissues (non-treated EcEnd versus non-treated EuSham, $P = 0.0221$; versus EushamMet $P = 0,0010$); this was confirmed through computer-assisted analysis of the fibrosis to total area ratio (FIGURE 2ii). Metformin treatment restored the levels of fibrosis in the tissues to those found in the Sham groups in non-mated animals (FIGURE 2ii, Supplementary Table 2). When the ectopic tissue from non-mated mice was compared with that from pregnant mice, a significant decrease in fibrosis in pregnant EcEndMet mice was only observed relative to non-mated EcEnd mice ($P = 0.0187$; FIGURE 2iii), again

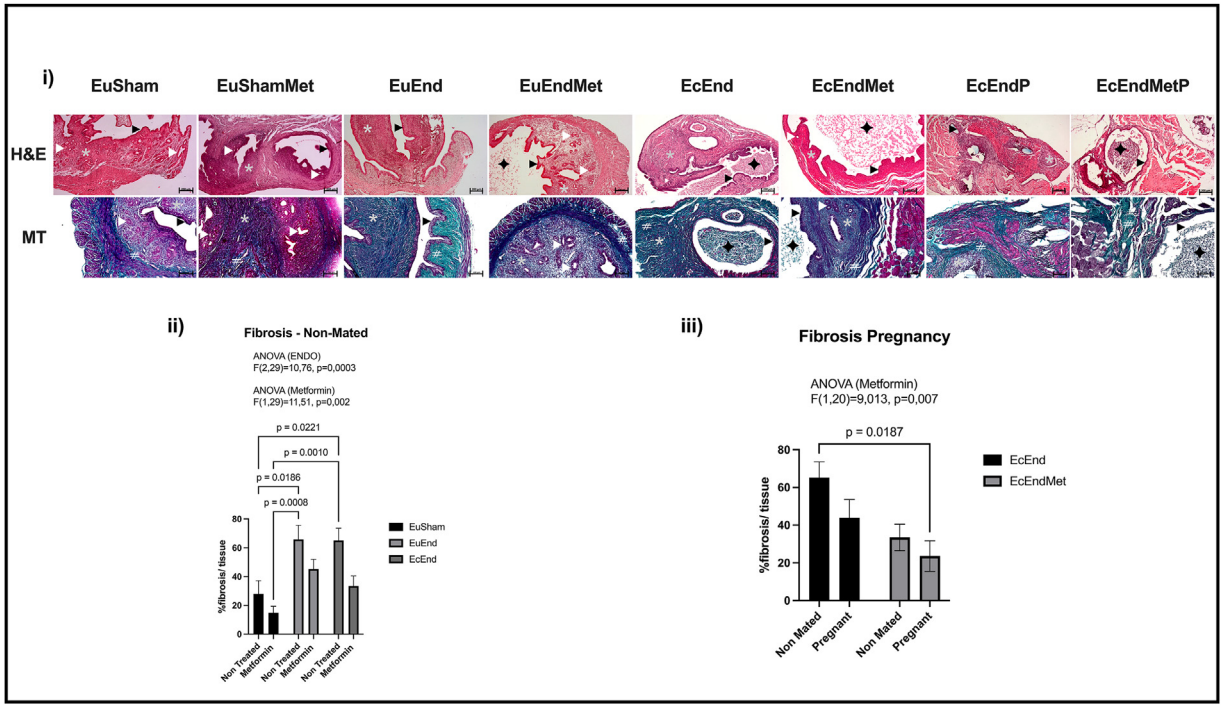

FIGURE 2 Endometriosis (ENDO) increases the fibrosis of endometrial tissue. (i) Representative images of haematoxylin and eosin (H&E; scale bar = 200 μm) and Masson trichrome (MT; scale bar = 100 μm) stained sections of eutopic and ectopic tissues, from the endometriosis experimental groups, either non-mated or pregnant. (ii, iii) Corresponding graphical depictions of the computer-assisted analysis of fibrosis in MT-stained sections. The statistical analysis employed two-way analysis of variance (ANOVA) followed by post-hoc analyses using Tukey's multiple comparisons tests. Values are presented as mean ± SEM. Significant *P*-values are shown in the figure, and all the *P*-values are shown in Supplementary Tables 2 and 3. White arrow heads indicate glands; black arrow heads indicated endometrial tissue epithelium; light grey asterisks denote stroma; white cardinal symbols show fibrosis; black stars indicate flaking cells. EuSham, eutopic tissue from sham-operated mice; EuShamMet, eutopic tissue from sham-operated mice treated with metformin; EuEnd, eutopic tissue from mice with endometriosis; EuEndMet, eutopic tissue from mice with endometriosis mice treated with metformin; EcEnd, ectopic tissue from mice with endometriosis; EcEndMet, ectopic tissue from mice with endometriosis mice treated with metformin; EcEndP, ectopic tissue from pregnant mice with endometriosis mice; EcEndMetP, ectopic tissue from pregnant mice with endometriosis mice treated with metformin.

with metformin not significantly decreasing fibrosis within the group of pregnant mice (Supplementary Table 3).

Ectopic endometrial tissue shows higher cell proliferation in non-mated mice but lower proliferation in pregnant mice

Specific markers of the cellular mechanisms involved in endometriosis progression, such as abnormal cell proliferation, oestrogen secretion, increased inflammation and oxidative stress, were analysed in the murine model of disease treated with metformin.

To assess the proliferative features of ectopic tissue, the cell proliferation marker PCNA was analysed through immunofluorescence in eutopic and ectopic samples of endometrial tissue. Labelling was noted in the nuclei of the cells, particularly in epithelial cells, from all the analysed tissues (FIGURE 3Ai).

In addition, a band of approximately 36 kDa corresponding to PCNA was identified by western blotting (FIGURE 3Aiv, vii). Two-way ANOVA analysis showed an endometriosis effect in tissues from non-mated mice, as well as a pregnancy effect in the ectopic tissues analysed. Semi-quantification of PCNA (FIGURE 3Av) revealed an increase in the EcEnd group compared with the EuSham, EuShamMet and EuEndMet mice (all $P \leq 0{,}0231$). No differences were found, however, when comparing EcEnd with EuEnd ($P = 0{,}0893$), or EcEndMet with EuSham (p=0,0952), EuShamMet ($P = 0{,}0704$) or EuEndMet ($P = 0{,}0901$) (FIGURE 3Av, Supplementary Table 4). On the other hand, a significant decrease in PCNA expression was found in both the pregnant EcEnd and pregnant EcEndMet mice compared with EcEnd mice (both $P \leq 0{,}0178$); FIGURE 3A–viii). These findings suggested that the extensive pro-proliferative and growth effect in ectopic tissue is hindered by pregnancy, independently of treatment with metformin.

Expression of CYP17a1 is increased by endometriosis but decreased by metformin treatment in ectopic endometrial tissue

CYP17a1, a marker of steroidogenesis, was detected in the analysed tissues by immunofluorescence (FIGURE 3Aii) and by western blotting with a band of approximately 56kDa (FIGURE 3Aiv, vii). Two-way ANOVA showed that endometriosis had an effect on CYP17a1 expression in tissues from non-mated animals, and that pregnancy also had an effect on this protein. On the other hand, the effect of metformin in these tissues did not reach significance. The levels of CYP17a1 increased in EuEnd compared with EuSham mice ($P = 0{,}0228$) but decreased with metformin treatment in EcEndMet mice ($P = 0{,}0170$; FIGURE 3Avi). There was a decrease in CYP17a1 levels in ectopic tissue from pregnant mice treated with metformin compared with both treated and non-treated ectopic tissues from non-mated mice (both $P \leq 0{,}0203$; FIGURE 3Aix).

Inflammatory cell markers and NFκB were increased by metformin treatment in non-mated but not pregnant mice

Dual immunolabelling of F4/80 (a macrophage marker) and galectin-3 (a molecule involved in the inflammatory response that is expressed by immune cells) was carried out to elucidate the inflammatory features in endometriosis. Labelling for both proteins was noticed in the stroma cells of all the tissues studied but was absent from the epithelia. Both labels had a diffuse, scattered pattern but showed clusters of positive cells in some sections (FIGURE 3Bi). In addition, F4/80 was identified as several bands ranging from 75 to 200 kDa on western blotting (FIGURE 3Bii, vi).

Two-way ANOVA analysis revealed that both endometriosis and metformin had an effect in tissues from non-mated mice, and that both metformin and pregnancy had an effect in ectopic tissues. F4/80 increased in EuEndMet mice compared with the EuEnd ($P = 0.0002$) and EuSham ($P = 0{,}0146$) groups and also with non-treated EcEnd mice ($P < 0.0001$). In ectopic tissue from EcEndMet animals there was a strong tendency towards an increased expression of F4/80 relative to EcEnd mice ($P = 0{,}0725$; FIGURE 3Biii). The variation between these two groups reached significance when the F4/80 expression levels were normalized to those of the ectopic tissues from the End group in the comparison between ectopic tissues from non-mated and pregnant animals. In this case, not only did metformin increase F4/80 levels in non-mated mice ($P = 0.0037$), but an equivalent trend was also observed in pregnant mice ($P = 0{,}1611$). A significant decrease was observed when comparing pregnant EcEndMet with pregnant EcEnd mice ($P = 0{,}0011$; FIGURE 3Bvii).

Galectin-3 was identified by western blotting as a band of approximately 30 kDa (FIGURE 3Bii, vi). Two-way ANOVA revealed that metformin had an effect on the tissues of non-mated animals, and in the comparison between ectopic tissues, pregnancy had an effect while the effect of metformin almost reached significance. In line with the data relative to F4/80 and NFκB (FIGURE 3Bv), metformin increased galectin-3 levels in ectopic tissue (EcEndMet) compared with all the other tissues studied: EuSham ($P < 0.0001$), EuShamMet ($P < 0.0001$), EuEnd ($P = 0.0002$), EuEndMet ($P = 0.0031$) and EcEnd ($P = 0.0039$) (FIGURE 3Biv). In ectopic tissues from non-mated and pregnant mice, decreased levels of galectin-3 were observed when comparing non-mated EcEndMet mice with their non-treated counterparts ($P = 0{,}0291$) and with both ectopic tissues in pregnant EcEnd ($P = 0{,}0099$) and pregnant EcEndMet ($P = 0{,}0099$) mice (FIGURE 3Bviii).

Regarding NFκB, a transcription factor involved in the inflammatory response, a band of approximately 65 kDa was identified (FIGURE 3Bii, vi). Two-way ANOVA showed that metformin had an effect on the tissues of non-mated mice and that both metformin and pregnancy showed an effect when comparing ectopic tissues. The quantification of NFκB concentrations showed an increase in the ectopic tissue of animals treated with metformin (EcEndMet) compared with all the tissues from the non-treated groups: EuSham ($P = 0{,}0062$), EuEnd ($P = 0{,}0070$) and EcEnd ($P = 0{,}0293$) (FIGURE 3Bv). Within the ectopic tissues, non-mated animals treated with metformin presented increased NFκB concentrations relative to their non-treated counterparts ($P = 0.0038$) and to both groups of pregnant mice: pregnant EcEnd ($P = 0.0025$) and pregnant EcEndMet ($P = 0{,}0177$) mice (FIGURE 3Bix).

Metformin increased the expression of antioxidant defence enzymes in the ectopic endometrial tissue of non-mated mice

The oxidative response was evaluated by western blotting quantification of HO-1 and GPX-1, the enzymes with anti-oxidative properties. HO-1 was identified as a band of approximately 28 kDa (FIGURE 3Ci, iv).

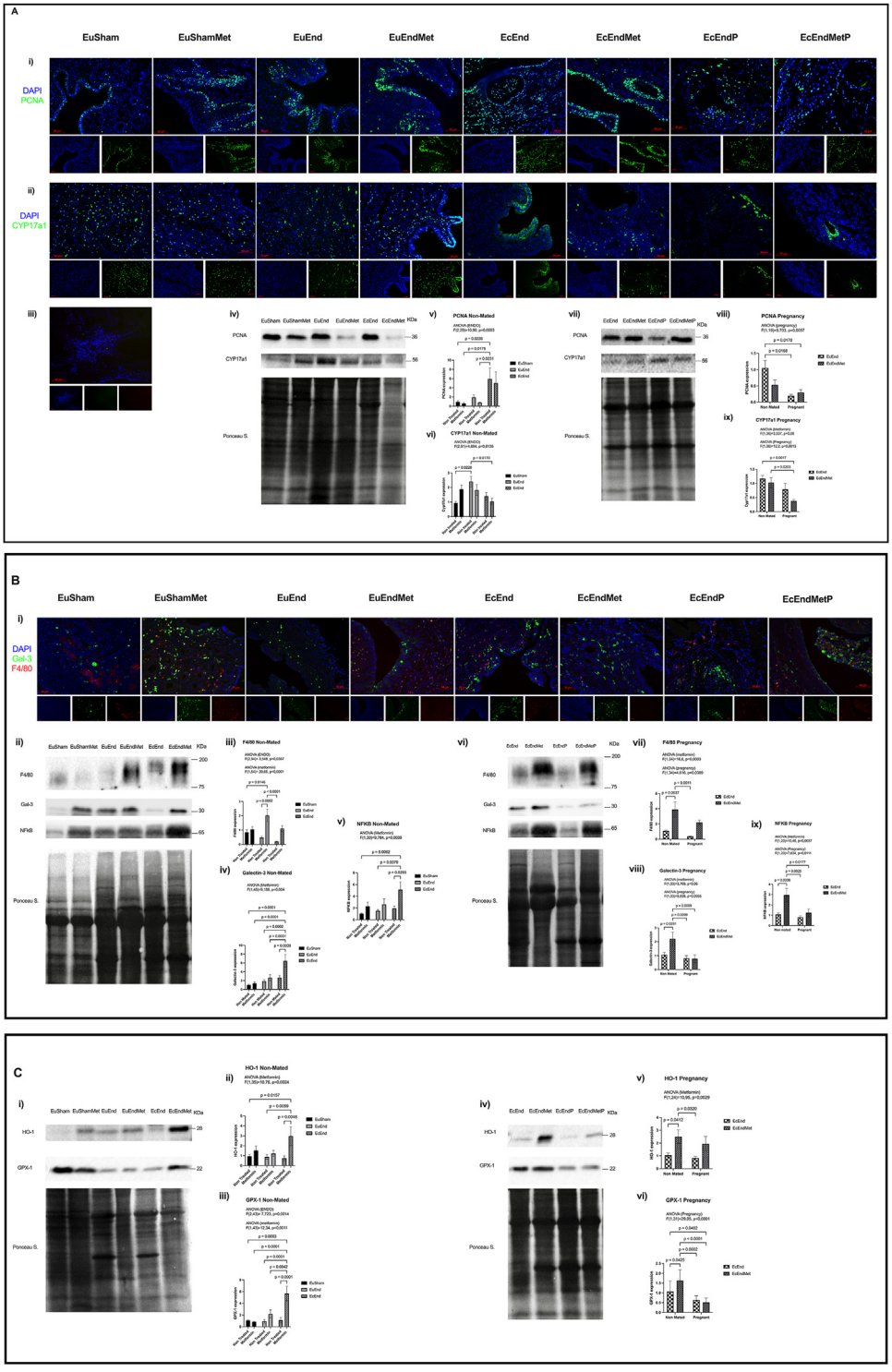

FIGURE 3 Metformin increases inflammatory markers and antioxidative defences in ectopic tissue from non-mated mice, while endometriosis (ENDO) impacts cell proliferation and oestrogen production in the tissues. (A) Representative immunofluorescence images: (i) green labelling for proliferating cell nuclear antigen (PCNA); (ii) green labelling for cytochrome P450 17a1 (CYP17a1); and (iii) negative control. Nuclei are labelled in blue (4′,6-diamidino-2-phenyl-indole [DAPI]), and the corresponding single-channels are shown below the merged images. Scale bars = 50 μm. (iv, vii) Representative images of PCNA and CYP17a1 bands detected by western blotting and representative membrane stained with Ponceau S. Analysis of tissues from non-mated mice compared with pregnant mice was carried out in separate blots. (v, vi, viii, ix) Quantitative analysis of PCNA (v, viii) and CYP17a1 (vi, ix) between treatment groups for non-mated mice and ectopic tissues from pregnant mice compared with their non-mated counterparts. (B) (i) Representative images of immunofluorescence dual labelling for F4/80 (red) and galectin-3 (green), with the corresponding individual channels below each image. Nuclei were labelled blue with DAPI. Scale bars = 50 μm. (ii, vi) Representative images of F4/80, galectin-3 and nuclear factor kappa B (NFκB) bands detected by western blotting and the corresponding Ponceau S-stained membrane used as a control of loading. (iii, v, vii, ix) Quantitative analysis of F4/80 (iii, vii), galectin-3 (iv, viii) and NFκB (v, ix) between groups of non-mated mice and ectopic tissues from pregnant mice compared with

Two-way ANOVA showed that metformin had an effect on both the tissues of non-mated mice and in the comparison of ectopic tissues. In line with the data observed for the previously analysed proteins, an increase in HO-1 expression in the EcEndMet group was found compared with all the tissues from non-treated animals: EuSham ($P = 0{,}0157$), EuEnd ($P = 0{,}0059$) and EcEnd ($P = 0{,}0048$) (FIGURE 3Cii). When looking at the ectopic tissues to analyse the effect of pregnancy, this increase was also observed in non-mated mice treated with metformin relative to non-treated animals ($P = 0{,}0412$). In addition, pregnant EcEnd mice presented lower levels of HO-1 than EcEndMet mice ($P = 0{,}0320$). Metformin treatment in pregnant mice, compared with their non-treated counterparts, did not increase HO-1 expression ($P = 0{,}2522$; FIGURE 3Cv).

GPX-1, identified as a band of approximately 22 kDa (FIGURE 3Ci, iv), presented a similar variation between the groups to that observed for HO-1. Two-way ANOVA indicated that metformin had an effect on the tissues of non-mated mice, and pregnancy was shown to have effect when comparing ectopic tissues. EcEndMet tissue showed higher GPX-1 expression than EuSham, EuShamMet, EuEnd, EuEndMet and EcEnd tissue (all $P \leq 0{,}0042$; FIGURE 3Ciii). When comparing the ectopic tissues, increased GPX-1 expression was observed in metformin-treated non-mated animals relative to non-treated mice and to both groups of pregnant mice (all $P \leq 0{,}0425$). In addition, a decrease in GPX-1 expression was found in tissues from pregnant EcEndMet mice compared with non-mated EcEnd mice ($P = 0{,}0425$; FIGURE 3Cvi).

Metformin restores the reduction of fertility in endometriosis

As expected, recipient animals, including those with surgically induced endometriosis, maintained the functional integrity of the reproductive system, which was crucial for the further evaluation of fertility rates. In all groups of pregnant mice the uteruses with fetuses were visible at the 18th day end-point (FIGURE 4i–iv; the image relative to the ShamMet group is not shown). Adhesions and vascularized implants were still visible in End mice (FIGURE 4ii, iii) and, as observed before pregnancy, implants in EndMet mice were observed clearer than those in End animals (FIGURE 4iv).

Endometriosis is associated with infertility in women, and the present mouse model of disease successfully replicated this aspect, as a reduction in the average number of fetuses per pregnant mouse was observed in the End group compared with the Sham group ($P = 0{,}0034$; FIGURE 4v). It was also demonstrated that treatment with metformin played an effective role in restoring the average number of fetuses to levels similar to those found in the Sham group (Supplementary Table 18). Notably, there was a statistically significant increase in the average number of fetuses per pregnant mouse in the EndMet group compared with the End group ($P = 0{,}0295$; FIGURE 4v). The number of reabsorptions (FIGURE 4i–iv) showed no differences between the groups (FIGURE 4-vi; Supplementary Table 19) .

DISCUSSION

Endometriosis is a leading cause of infertility in women (*Guo, 2009*; *Lin et al., 2018*) and a painful recurrent condition requiring frequent analgesic and long-term hormone-based treatments. These have the advantage of mitigating much of the pain but at the expense of unwanted side effects, suppression of the menstrual cycle and decisions to postpone pregnancy. Thus, innovative long-term therapeutic approaches that mitigate the symptoms and progression of endometriosis, preserve women's reproductive function and can be used in pregnancy are a still unmet need (*Rafique and Decherney, 2017*; *Taylor et al., 2021*).

Despite endometriosis being a natural disease of women and other primates, this has not precluded the use of other mammals including rodents as experimental models of endometriosis. In general, these animal models aim to recapitulate the natural history of the human disorder, its pathophysiology and its related consequences, notably the reduced fertility (*Bilotas et al., 2015*; *Cohen et al., 2015*; *Flores et al., 2007*; *Greaves et al., 2014*; *Hayashi et al., 2020*; *Park et al., 2022*; *Rosa-E-Silva et al., 2019*; *Sharpe-Timms et al., 2020*; *Stilley et al., 2009*). The experimental models also provide a means to study novel pharmacological interventions, notably their functional and structural consequences, aiming for use in humans.

In the current model, endometriosis was established by the peritoneal implantation of allogenic endometrial grafts; the pharmacological intervention was the antioxidant and antidiabetic drug metformin. The use of a model in an animal that does not naturally develop endometriosis is a limitation of the study; similarly, the dose of metformin per animal (70 mg/kg per day) was calculated based on the average ingestion of water by the group. This is lower than the standard dose of metformin used in human treatment (500 mg twice a day), and after adjustment to rodents corresponds to 200 mg/kg per day (*Nair and Jacob, 2016*). Considering that the animal model of endometriosis does not present insulin resistance and that excessive doses of medication should be avoided in pregnancy, a lower dose of metformin was selected. The use of metformin in the control of gestational diabetes has been demonstrated to be safe for both women and fetuses in doses of 500 mg to 2.5 g per day (*Ainuddin et al., 2015*; *Beyuo et al., 2015*).

The concentrations of total cholesterol, HLD-C, LDL-C and glucose in the blood did not differ significantly when the groups were compared, indicating that the subtherapeutic dose of metformin employed did not change glucose and lipid metabolism.

Endometrial implants successfully engrafted in the peritoneum and thrived, as verified by ultrasonography and upon

their non-mated counterparts. (C) (i, iv) Representative images of HO-1 and GPX-1 bands detected by western blotting and corresponding Ponceau S-stained membranes used as a control of loading. (ii, iii, v, vi) Quantitative analysis of heme oxygenase (HO-1; ii, v) and glutathione peroxidase (GPX-1; iii, vi) between groups of non-mated mice and ectopic tissues from pregnant mice compared with their non-mated counterparts. The statistical analysis employed two-way analysis of variance (ANOVA) followed by post-hoc analyses using Tukey's multiple comparisons tests. Values are presented as mean ± SEM. Significant *P*-values are shown in the figure, and all the *P*-values are shown in Supplementary Tables 4–17. EuSham, eutopic tissue from sham-operated mice; EuShamMet, eutopic tissue from sham-operated mice treated with metformin; EuEnd, eutopic tissue from mice with endometriosis; EuEndMet, eutopic tissue from mice with endometriosis mice treated with metformin; EcEnd, ectopic tissue from mice with endometriosis; EcEndMet, ectopic tissue from mice with endometriosis mice treated with metformin; EcEndP, ectopic tissue from pregnant mice with endometriosis mice; EcEndMetP, ectopic tissue from pregnant mice with endometriosis mice treated with metformin.

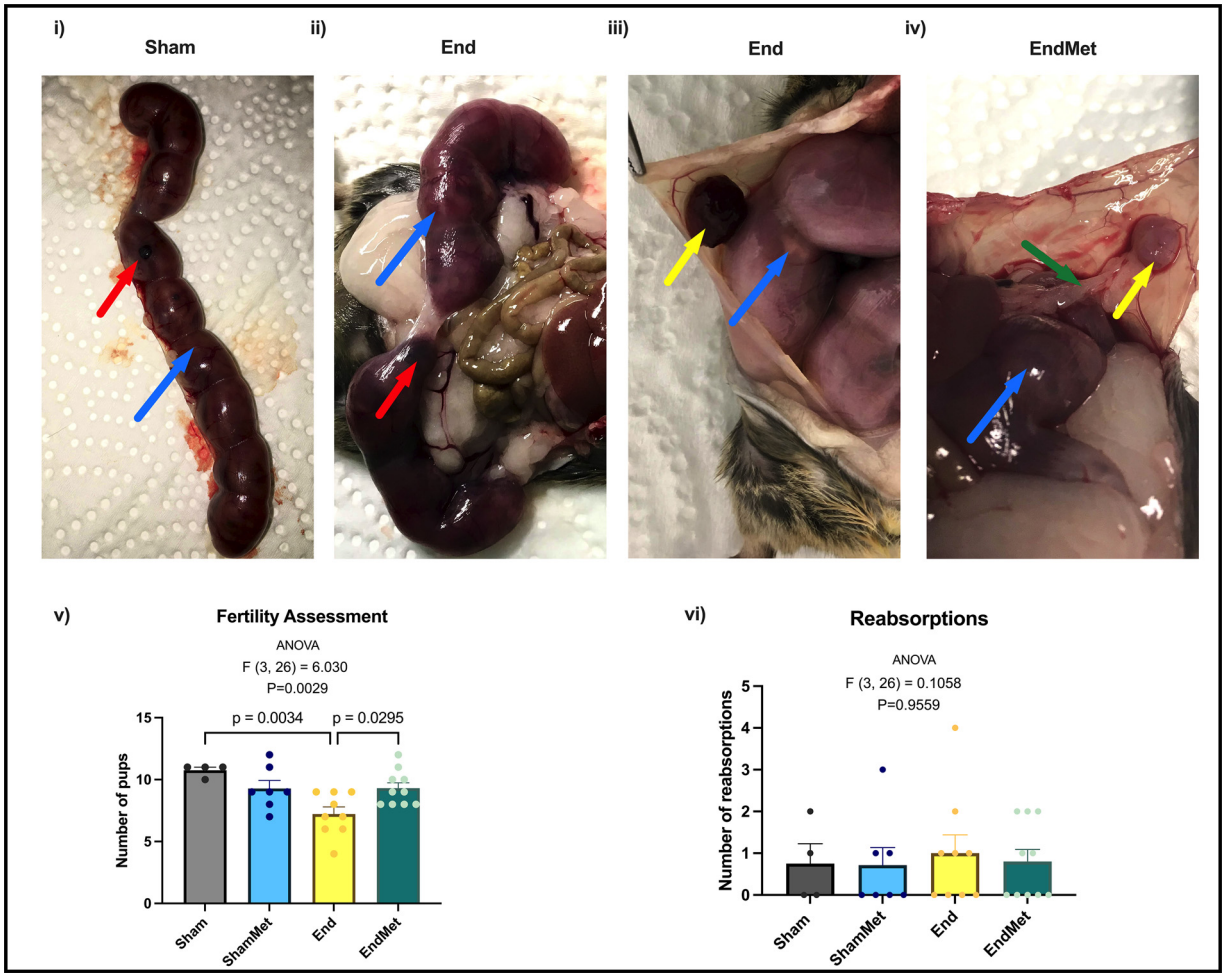

FIGURE 4 Metformin reduces endometriosis (ENDO) and restores fertility in the mouse model of disease. Representative uteri from pregnant mice at the 18th day after the mating end-point: (i) Sham group; (ii, iii) End group; and (iv) EndMet group. Blue arrows indicate a visible fetus; red arrows denote reabsorption sites; the green arrow indicates adhesions; yellow arrows show vascularized implants. (v) Graphical depiction of fertility assessment by the number of fetuses per pregnant female mouse between the groups. (vi) Graphical depiction of the number of reabsorptions per pregnant mouse between the groups. The statistical analysis employed one-way analysis of variance analysis of variance (ANOVA) followed by post-hoc analyses using Tukey's multiple comparisons tests. Values are presented as mean ± SEM, with the points showing individual mice. Significant *P*-values are shown in the figure, and all the *P*-values are shown in Supplementary Tables 18 and 19. Sham, sham-operated mice; ShamMet, sham-operated mice treated with metformin; End, mice with endometriosis; EndMet, mice with endometriosis mice treated with metformin.

visual inspection after laparotomy. Tissue PCNA evaluation by the current group and others (*Wang et al., 2023*) provided additional support for implant growth. A major finding in the ultrasound assessment was that metformin treatment restrained the growth of the implants, in agreement with previous reports in rodents (*Cheng et al., 2022*; *Oner et al., 2010*; *Sapmaz et al., 2022*; *Yilmaz et al., 2010*). Moreover, on inspection, metformin also improved the appearance of the implants, as they were clearer in colour, in contrast to lesions in untreated animals that exhibited a darker, brown bloody appearance, resembling 'chocolate cysts' similar to those frequently observed in the ovaries of women with endometriosis.

It is well established that the progression of endometriosis depends on oestrogen (*Rizner, 2009*), and that metformin is a known regulator of its synthesis and secretion (*Cheng et al., 2022*; *Zhang et al., 2017*). Oestradiol and other sex hormones predominantly in the ovary require the activity of the steroidogenic CYP17a1 enzyme (*Burris-Hiday and Scott, 2021*). The variation in CYP17a1 expression in the uterine tissue suggests that it may be a modulator of local (endometrial) response in endometriosis. In fact, an enhanced expression of CYP17a1 was observed in the eutopic endometrial tissue of non-treated endometriotic mice compared with controls, but not in the ectopic endometrial tissue, emphasizing the relevance of specific cellular environments. In contrast, CYP17a1 expression evidenced a downward response to metformin in both eutopic and ectopic endometrial tissue. This change suggests that a decrement in oestradiol is the likely mechanism for the growth restriction of endometriotic implants and indicates that metformin has a preventive effect on disease progression.

In mice with endometriosis there was an increase in fibrosis in both eutopic and ectopic tissues. The finding is a frequent occurrence following prolonged inflammation, itself a hallmark of the human disease (*Itoga et al., 2003*; *Viganò et al., 2020*), and is involved in the

establishment and progression of endometriotic lesions (*Maybin et al., 2011*). Interestingly, following metformin administration, there was a trend for the fibrosis to decrease, probably reflecting a particular ability of the drug (*Wu et al., 2021*), which may not be similar for every tissue. In fact, a decrease in fibrosis has been reported in ovarian and uterine tissue in a rat model of metformin-treated polycystic ovary syndrome (*Zhang et al., 2013*), but not in the heart in an endometriosis mouse model (*Martins et al., 2022*), suggesting a relationship to the turnover capacity of cells in the different tissues, which is very marked when one compares the dynamic endometrial epithelium and stroma, and the cellularly stable myocardium.

Inflammatory pathways are extensive and complex, and recruit a variety of cells and molecules that converge to the site of inflammation, where they attract more cells and molecules. Macrophage secretory products and galectin-3 are major players in inflammation (*Capobianco and Rovere Querini, 2013*; *Hogg et al., 2020*; *Lousse et al., 2008*; *Yamashita et al., 2022*). Galectin-3, an inflammation-associated protein and marker of surveillance cells, works also as chemoattractant for immune cells, including macrophages, and has been related to the formation of tissue fibrosis (*Hisrich et al., 2020*). However, in implants and sham-operated uteri at timepoint 3 in the current study, galectin-3 and NFκB expression were similar; in addition, F4/80, a major macrophage marker, had a particularly low level of expression in implants. This low expression profile suggests that, despite the important role of macrophages in inflammation, the tissue may have entered a condition of poorer response, similar to that found in kidney, where F4/80 exhibits a dynamic change from pro-inflammatory to anti-inflammatory action (*Kim et al., 2010*), while contributing to cell migration (*McKnight and Gordon, 1996*; *Stacey et al., 2000*) or adhesion of macrophages to the extracellular matrix or other cell types.

In this study, the low-response condition appears to have changed when metformin was added. In fact, galectin-3, NFkB and F4/80 exhibited all an upward trend, suggesting that the tissues had returned to an inflammatory-like state, which is important to drive the tissues back to a resolution. Nevertheless, tissue-specific properties may again underlie the variety of responses observed. For example, metformin treatment led to an increase in F4/80 in eutopic tissue, a finding that aligns with a previous demonstration where an increase in F4/80+ cell content in the mouse liver was observed after metformin treatment (*Woo et al., 2014*), while galectin-3 and NFκB are augmented in ectopic tissue. In contrast, systemic levels of galectin-3 decreased (*Weigert et al., 2010*), further supporting the view that galactin-3 often plays a dual role, as a pro-inflammatory but also an anti-inflammatory molecule (*Hisrich et al., 2020*). This versatility is further exemplified by the ability of galectin-3 to scavenge advanced glycosylated end-products, which are irreversibly glycated under pro-oxidative conditions (*Hogg et al., 2020*; *Pricci et al., 2000*; *Vlassara et al., 1995*). By altering gene expression in favour of the expression of anti-inflammatory molecules and excessive cell apoptosis (*Lawrence, 2009*; *Pereira and Oakley, 2008*), NFκB promotes inflammation resolution (*Lawrence et al., 2001*).

The findings discussed so far indicate that, in this model, endometrial implants become established and grow in an oestradiol-dependent environment and cause local inflammation, mimicking the natural disease. More importantly, metformin is able to favour the reversal of these lesions, leading to a beneficial reduction in fibrosis and implant size.

Endometriosis is recognized as a pro-oxidative disease (*Donnez et al., 2016*), which stems from an increment in the production of pro-oxidative molecules and/or a down-regulation of antioxidative defences. In this setting, GPX-1 serves as safeguard for the cells against oxidative damage. In fact, apart from modulating processes such as metabolism, mitochondrial function, growth and apoptosis, GPX-1 has the capacity to adjust intracellular concentrations of hydrogen peroxide and maintain the overall intracellular redox balance (*Lubos et al., 2011*). Additionally, HO-1, traditionally seen as an adaptive cellular response to oxidative stress toxicity, has gained recognition for its significant immunomodulatory and anti-inflammatory roles (*Campbell et al., 2021*).

In this study, both HO-1 and GPX-1 exhibited a similar level of expression at baseline in the control animals and even in eutopic and ectopic tissues in mice with endometriosis. However, upon metformin administration, the ectopic samples from the endometriosis group showed a significant increase in HO-1 and GPX-1 expression, paralleling the changes in the inflammation-associated molecules NFκB and galectin-3. In line with the current data, metformin has been recognized to activate the antioxidative response in a mouse model of diabetes (*Zhang et al., 2022*). In addition, a plant-derived flavonoid, naringenin, was shown to improve endometriosis in rats through increasing HO-1 expression in the lesions (*Kapoor et al., 2019*). In respect to the GPX-1 results, consistency with previous studies was found in terms of the its expression in the cardiac tissue of in a mouse model of endometriosis and a rat model of diabetes (*Felgueiras et al., 2022*), and also in the brain of rats (*Obafemi et al., 2020*). Thus, in addition to reversing some of the consequences associated with endometriosis, such as implant growth and local fibrosis, metformin led to an up-regulation of antioxidative enzymatic defences, further limiting the progression and effects of the endometriosis.

An important result was noticed in pregnancy as this affected oestradiol and cholesterol concentrations in every study group. The increase in oestradiol is a recognized change in human pregnancy, here verified in pregnant mice. In contrast, the reduction in cholesterol concentration in pregnant mice (*Sweeney et al., 2006*), while conflicting with the findings in humans (*Green, 1966*; *Ogura et al., 2002*), may reflect a distinct means of cholesterol processing. Indeed, the main supplier of cholesterol to the tissues in humans is LDL-C, whereas in rodents it is HDL-C (*Grummer and Carroll, 1988*).

Pregnancy is an important issue in the setting of endometriosis. The assessment of ectopic endometriotic tissue from pregnant mice receiving metformin showed a decrease in expression of PCNA, CYP17a1 and GPX1 relative to non-mated EcEnd animals, and CYP17a1, galectin-3, NFκB and GPX-1 relative to non-mated EcEndMet animals. This similarity in the response of these molecules emphasizes the importance of pregnancy and indicates that it overrode the endometriotic condition and buffered its effects.

As a corollary of the beneficial consequences of metformin administration, the assessment of fertilization revealed a most important finding. After the significant reduction in

the number of fetuses per pregnant mouse in the group with induced endometriosis compared with their sham-operated counterparts, also observed by Cohen and collaborators (*Cohen et al., 2015*), a reversal of infertility was found in the group of mice with endometriosis that were treated with metformin. This evidence marks the first documented reversal of endometriosis-associated infertility with metformin in a mouse model despite a previous report of an equivalent effect with the natural compound oleuropein (*Park et al., 2022*).

In conclusion, the current study establishes a mouse model illustrating the reversal of infertility associated with endometriosis through metformin treatment, probably through its anti-inflammatory properties manifested in pregnancy. The subtherapeutic dose employed, tailored to this animal model, demonstrated promising outcomes. Although metformin showed consistency of action in the oxidation response pathways, its impact on inflammatory pathways necessitates further exploration. These findings constitute valuable insights into the potential benefits and complexities of metformin in the context of endometriosis, paving the way for future research and clinical considerations.

DATA AVAILABILITY

Data will be made available on request.

ACKNOWLEDGEMENTS

BioRender was used in the construction of FIGURE 1 and the graphical abstract (Neto, A., 2024, https://BioRender.com/d99y595).

FUNDING

The contract DL57/2016/CP1355/CT0009 of A. R. Rodrigues was funded by FCT – Fundação para a Ciência e Tecnologia – Portugal.

SUPPLEMENTARY MATERIALS

Supplementary material associated with this article can be found in the online version at doi:10.1016/j.rbmo.2024.104474.

REFERENCES

Ainuddin, J.A., Karim, N., Zaheer, S., Ali, S.S., Hasan, A.A., 2015. Metformin treatment in type 2 diabetes in pregnancy: an active controlled, parallel-group, randomized, open label study in patients with type 2 diabetes in pregnancy. J Diabetes Res 2015, 325851. https://doi.org/10.1155/2015/325851.

Alderman, 3rd, M.H., Yoder, N., Taylor, H.S., 2017. The Systemic Effects of Endometriosis. Semin Reprod Med 35 (3), 263–270. https://doi.org/10.1055/s-0037-1603582.

Beyuo, T., Obed, S.A., Adjepong-Yamoah, K.K., Bugyei, K.A., Oppong, S.A., Marfoh, K., 2015. Metformin versus Insulin in the Management of Pre-Gestational Diabetes Mellitus in Pregnancy and Gestational Diabetes Mellitus at the Korle Bu Teaching Hospital: A Randomized Clinical Trial. PLoS One 10 (5), e0125712. https://doi.org/10.1371/journal.pone.0125712.

Bilotas, M.A., Olivares, C.N., Ricci, A.G., Baston, J.I., Bengochea, T.S., Meresman, G.F., Barañao, R.I., 2015. Interplay between Endometriosis and Pregnancy in a Mouse Model. PLoS One 10 (4), e0124900. https://doi.org/10.1371/journal.pone.0124900.

Burris-Hiday, S.D., Scott, E.E., 2021. Steroidogenic cytochrome P450 17A1 structure and function. Molecular and Cellular Endocrinology 528, 111261. https://doi.org/10.1016/j.mce.2021.111261.

Campbell, N.K., Fitzgerald, H.K., Dunne, A., 2021. Regulation of inflammation by the antioxidant haem oxygenase 1. Nature Reviews Immunology 21 (7), 411–425. https://doi.org/10.1038/s41577-020-00491-x.

Capobianco, A., Rovere Querini, P., 2013. Endometriosis, a disease of the macrophage [Review]. Frontiers in Immunology 4. https://doi.org/10.3389/fimmu.2013.00009.

Cheng, J., Li, C., Ying, Y., Lv, J., Qu, X., McGowan, E., Lin, Y., Zhu, X., 2022. Metformin Alleviates Endometriosis and Potentiates Endometrial Receptivity via Decreasing VEGF and MMP9 and Increasing Leukemia Inhibitor Factor and HOXA10. Front Pharmacol 13, 750208. https://doi.org/10.3389/fphar.2022.750208.

Clower, L., Fleshman, T., Geldenhuys, W.J., Santanam, N., 2022. Targeting Oxidative Stress Involved in Endometriosis and Its Pain. Biomolecules 12 (8), 1055. https://www.mdpi.com/2218-273X/12/8/1055.

Coccia, M.E., Nardone, L., Rizzello, F., 2022. Endometriosis and Infertility: A Long-Life Approach to Preserve Reproductive Integrity. International Journal of Environmental Research and Public Health 19 (10), 6162. https://www.mdpi.com/1660-4601/19/10/6162.

Cohen, J., Ziyyat, A., Naoura, I., Chabbert-Buffet, N., Aractingi, S., Darai, E., Lefevre, B., 2015. Effect of induced peritoneal endometriosis on oocyte and embryo quality in a mouse model. J Assist Reprod Genet 32 (2), 263–270. https://doi.org/10.1007/s10815-014-0390-1.

Donnez, J., Binda, M.M., Donnez, O., Dolmans, M.-M., 2016. Oxidative stress in the pelvic cavity and its role in the pathogenesis of endometriosis. Fertility and Sterility 106 (5), 1011–1017. https://doi.org/10.1016/j.fertnstert.2016.07.1075.

Evans, M.B., Decherney, A.H., 2017. Fertility and Endometriosis. Clin Obstet Gynecol 60 (3), 497–502. https://doi.org/10.1097/grf.0000000000000295.

Felgueiras, R., Neto, A.C., Rodrigues, A.R., Gouveia, A.M., Almeida, H., Neves, D., 2022. Anti-oxidant effect of metformin through AMPK/SIRT1/PGC-1α/SIRT3– independent GPx1 expression in the heart of mice with endometriosis. Hormone Molecular Biology and Clinical Investigation 43 (4), 405–414. https://doi.org/10.1515/hmbci-2022-0039.

Flores, I., Rivera, E., Ruiz, L.A., Santiago, O.I., Vernon, M.W., Appleyard, C.B., 2007. Molecular profiling of experimental endometriosis identified gene expression patterns in common with human disease. Fertil Steril 87 (5), 1180–1199. https://doi.org/10.1016/j.fertnstert.2006.07.1550.

Greaves, E., Cousins, F.L., Murray, A., Esnal-Zufiaurre, A., Fassbender, A., Horne, A.W., Saunders, P.T., 2014. A novel mouse model of endometriosis mimics human phenotype and reveals insights into the inflammatory contribution of shed endometrium. Am J Pathol 184 (7), 1930–1939. https://doi.org/10.1016/j.ajpath.2014.03.011.

Green, J.G., 1966. Serum cholesterol changes in pregnancy. American Journal of Obstetrics and Gynecology 95 (3), 387–393. https://doi.org/10.1016/0002-9378(66)90123-2.

Grummer, R.R., Carroll, D.J., 1988. A Review of Lipoprotein Cholesterol Metabolism: Importance to Ovarian Function. Journal of Animal Science 66 (12), 3160–3173. https://doi.org/10.2527/jas1988.66123160x.

Guo, S.-W., 2009. Recurrence of endometriosis and its control. Human Reproduction Update 15 (4), 441–461. https://doi.org/10.1093/humupd/dmp007.

Hayashi, S., Nakamura, T., Motooka, Y., Ito, F., Jiang, L., Akatsuka, S., Iwase, A., Kajiyama, H., Kikkawa, F., Toyokuni, S., 2020. Novel ovarian endometriosis model causes infertility via iron-mediated oxidative stress in mice. Redox Biology 37, 101726. https://doi.org/10.1016/j.redox.2020.101726.

Hisrich, B.V., Young, R.B., Sansone, A.M., Bowens, Z., Green, L.J., Lessey, B.A., Blenda, A.V., 2020. Role of Human Galectins in Inflammation and Cancers Associated with Endometriosis. Biomolecules 10 (2), 230. https://www.mdpi.com/2218-273X/10/2/230.

Hogg, C., Horne, A.W., Greaves, E., 2020. Endometriosis-Associated Macrophages: Origin, Phenotype, and Function [Review]. Frontiers in Endocrinology 11. https://doi.org/10.3389/fendo.2020.00007.

Inhorn, M.C., Patrizio, P., 2015. Infertility around the globe: new thinking on gender, reproductive technologies and global movements in the 21st century. Human Reproduction Update 21 (4), 411–426. https://doi.org/10.1093/humupd/dmv016.

Itoga, T., Matsumoto, T., Takeuchi, H., Yamasaki, S., Sasahara, N., Hoshi, T., Kinoshita, K., 2003. Fibrosis and smooth muscle metaplasia in rectovaginal endometriosis. Pathology International 53 (6), 371–375. https://doi.org/10.1046/j.1440-1827.2003.01483.x.

Kapoor, R., Sirohi, V.K., Gupta, K., Dwivedi, A., 2019. Naringenin ameliorates progression of endometriosis by modulating Nrf2/Keap1/HO1 axis and inducing apoptosis in rats. The Journal of Nutritional Biochemistry 70, 215–226. https://doi.org/10.1016/j.jnutbio.2019.05.003.

Kim, M.-G., Su Boo, C., Sook Ko, Y., Young Lee, H., Yong Cho, W., Kyu Kim, H., Jo, S.-K., 2010. Depletion of kidney CD11c+ F4/80+ cells impairs the recovery process in ischaemia/reperfusion-

induced acute kidney injury. Nephrology Dialysis Transplantation 25 (9), 2908–2921. https://doi.org/10.1093/ndt/gfq183.
Lawrence, T., 2009. The nuclear factor NF-kappaB pathway in inflammation. Cold Spring Harb Perspect Biol 1 (6), a001651. https://doi.org/10.1101/cshperspect.a001651.
Lawrence, T., Gilroy, D.W., Colville-Nash, P.R., Willoughby, D.A., 2001. Possible new role for NF-kappaB in the resolution of inflammation. Nat Med 7 (12), 1291–1297. https://doi.org/10.1038/nm1201-1291.
Lin, Y.H., Chen, Y.H., Chang, H.Y., Au, H.K., Tzeng, C.R., Huang, Y.H., 2018. Chronic Niche Inflammation in Endometriosis-Associated Infertility: Current Understanding and Future Therapeutic Strategies. Int J Mol Sci 19 (8). https://doi.org/10.3390/ijms19082385.
Lousse, J.-C., Van Langendonckt, A., González-Ramos, R., Defrère, S., Renkin, E., Donnez, J., 2008. Increased activation of nuclear factor-kappa B (NF-κB) in isolated peritoneal macrophages of patients with endometriosis. Fertility and Sterility 90 (1), 217–220. https://doi.org/10.1016/j.fertnstert.2007.06.015.
Lubos, E., Loscalzo, J., Handy, D.E., 2011. Glutathione peroxidase-1 in health and disease: from molecular mechanisms to therapeutic opportunities. Antioxid Redox Signal 15 (7), 1957–1997. https://doi.org/10.1089/ars.2010.3586.
Martins, A.F., Neto, A.C., Rodrigues, A.R., Oliveira, S.M., Sousa-Mendes, C., Leite-Moreira, A., Gouveia, A.M., Almeida, H., Neves, D., 2022. Metformin Prevents Endothelial Dysfunction in Endometriosis through Downregulation of ET-1 and Upregulation of eNOS. Biomedicines 10 (11), 2782. https://www.mdpi.com/2227-9059/10/11/2782.
Maybin, J.A., Critchley, H.O.D., Jabbour, H.N., 2011. Inflammatory pathways in endometrial disorders. Molecular and Cellular Endocrinology 335 (1), 42–51. https://doi.org/10.1016/j.mce.2010.08.006.
McKnight, A.J., Gordon, S., 1996. EGF-TM7: a novel subfamily of seven-transmembrane-region leukocyte cell-surface molecules. Immunol Today 17 (6), 283–287. https://doi.org/10.1016/0167-5699(96)80546-9.
Nair, A.B., Jacob, S., 2016. A simple practice guide for dose conversion between animals and human. J Basic Clin Pharm 7 (2), 27–31. https://doi.org/10.4103/0976-0105.177703.
Obafemi, T.O., Olasehinde, O.R., Olaoye, O.A., Jaiyesimi, K.F., Adewumi, F.D., Adewale, O.B., Afolabi, B.A., 2020. Metformin/Donepezil combination modulates brain antioxidant status and hippocampal endoplasmic reticulum stress in type 2 diabetic rats. Journal of Diabetes & Metabolic Disorders 19 (1), 499–510. https://doi.org/10.1007/s40200-020-00541-0.
Ogura, K., Miyatake, T., Fukui, O., Nakamura, T., Kameda, T., Yoshino, G., 2002. Low-Density Lipoprotein Particle Diameter in Normal Pregnancy and Preeclampsia. Journal of Atherosclerosis and Thrombosis 9 (1), 42–47. https://doi.org/10.5551/jat.9.42.
Oner, G., Ozcelik, B., Ozgun, M.T., Serin, I.S., Ozturk, F., Basbug, M., 2010. The effects of metformin and letrozole on endometriosis and comparison of the two treatment agents in a rat model. Hum Reprod 25 (4), 932–937. https://doi.org/10.1093/humrep/deq016.
Park, Y., Cho, Y.J., Sung, N., Park, M.J., Guan, X., Gibbons, W.E., O'Malley, B.W., Han, S.J., 2022. Oleuropein suppresses endometriosis progression and improves the fertility of mice with endometriosis. J Biomed Sci 29 (1), 100. https://doi.org/10.1186/s12929-022-00883-2.
Pelch, K.E., Sharpe-Timms, K.L., Nagel, S.C., 2012. Mouse model of surgically-induced endometriosis by auto-transplantation of uterine tissue. J Vis Exp (59), e3396. https://doi.org/10.3791/3396.
Pereira, S.G., Oakley, F., 2008. Nuclear factor-κB1: Regulation and function. The International Journal of Biochemistry & Cell Biology 40 (8), 1425–1430. https://doi.org/10.1016/j.biocel.2007.05.004.
Pricci, F., Leto, G., Amadio, L., Iacobini, C., Romeo, G., Cordone, S., Gradini, R., Barsotti, P., Liu, F.-T., Di Mario, U., Pugliese, G., 2000. Role of galectin-3 as a receptor for advanced glycosylation end products. Kidney International 58, S31–S39. https://doi.org/10.1046/j.1523-1755.2000.07706.x.
Rafique, S., Decherney, A.H., 2017. Medical Management of Endometriosis. Clin Obstet Gynecol 60 (3), 485–496. https://doi.org/10.1097/grf.0000000000000292.
Rizner, T.L., 2009. Estrogen metabolism and action in endometriosis. Mol Cell Endocrinol 307 (1-2), 8–18. https://doi.org/10.1016/j.mce.2009.03.022.
Rosa-E-Silva, ACJS, Rosa-E-Silva, JC, Mamillapalli, R, Taylor, HS, 2019 Oct. Dose-Dependent Decreased Fertility in Response to the Burden of Endometriosis in a Murine *Model*. Reprod Sci 26 (10), 1395–1400. https://doi.org/10.1177/1933719119859438.
Samimi, M., Pourhanifeh, M.H., Mehdizadehkashi, A., Eftekhar, T., Asemi, Z., 2019. The role of inflammation, oxidative stress, angiogenesis, and apoptosis in the pathophysiology of endometriosis: Basic science and new insights based on gene expression. Journal of Cellular Physiology 234 (11), 19384–19392. https://doi.org/10.1002/jcp.28666.
Sapmaz, T., Coskun, G., Saker, D., Pence, H.H., Keles, P., Hayretdag, C., Kuras, S., Topkaraoglu, S., Erdem, E., Efendic, F., Sevgin, K., Tekayev, M., Polat, S., Sapmaz, E., Irkorucu, O., 2022. Effects of metformin, letrozole and atorvastatin on inflammation and apoptosis in experimental peritoneal and ovarian endometriosis in the rat. Pathology - Research and Practice 235, 153951. https://doi.org/10.1016/j.prp.2022.153951.
Sharpe-Timms, K.L., Nabli, H., Stilley, J.A.W., 2020. Identifying Mechanisms of Endometriosis-Associated Reduced Fecundity in a Rat Model: Novel Insights toward Understanding Human Infertility. Adv Anat Embryol Cell Biol 232, 9–24. https://doi.org/10.1007/978-3-030-51856-1_2.
Skorupskaite, K., Bhandari, H.M., 2021. Endometriosis and fertility. Obstetrics, Gynaecology & Reproductive Medicine 31 (5), 131–136. https://doi.org/10.1016/j.ogrm.2021.03.003.
Stacey, M., Lin, H.-H., Gordon, S., McKnight, A.J., 2000. LNB-TM7, a group of seven-transmembrane proteins related to family-B G-protein-coupled receptors. Trends in Biochemical Sciences 25 (6), 284–289. https://doi.org/10.1016/S0968-0004(00)01583-8.
Stilley, J.A., Woods-Marshall, R., Sutovsky, M., Sutovsky, P., Sharpe-Timms, K.L., 2009. Reduced fecundity in female rats with surgically induced endometriosis and in their daughters: a potential role for tissue inhibitors of metalloproteinase 1. Biol Reprod 80 (4), 649–656. https://doi.org/10.1095/biolreprod.108.073411.
Sweeney, T.R., Moser, A.H., Shigenaga, J.K., Grunfeld, C., Feingold, K.R., 2006. Decreased nuclear hormone receptor expression in the livers of mice in late pregnancy. American Journal of Physiology-Endocrinology and Metabolism 290 (6), E1313–E1320. https://doi.org/10.1152/ajpendo.00071.2005.
Takemura, Y., Osuga, Y., Yoshino, O., Hasegawa, A., Hirata, T., Hirota, Y., Nose, E., Morimoto, C., Harada, M., Koga, K., Tajima, T., Yano, T., Taketani, Y., 2007. Metformin suppresses interleukin (IL)-1beta-induced IL-8 production, aromatase activation, and proliferation of endometriotic stromal cells. J Clin Endocrinol Metab 92 (8), 3213–3218. https://doi.org/10.1210/jc.2006-2486.
Taylor, H.S., Kotlyar, A.M., Flores, V.A., 2021. Endometriosis is a chronic systemic disease: clinical challenges and novel innovations. Lancet 397 (10276), 839–852. https://doi.org/10.1016/s0140-6736(21)00389-5.
Viganò, P., Ottolina, J., Bartiromo, L., Bonavina, G., Schimberni, M., Villanacci, R., Candiani, M., 2020. Cellular Components Contributing to Fibrosis in Endometriosis: A Literature Review. J Minim Invasive Gynecol 27 (2), 287–295. https://doi.org/10.1016/j.jmig.2019.11.011.
Viollet, B., Guigas, B., Sanz Garcia, N., Leclerc, J., Foretz, M., Andreelli, F, 2012. Cellular and molecular mechanisms of metformin: an overview. Clin Sci (Lond) 122 (6), 253–270. https://doi.org/10.1042/cs20110386.
Vlassara, H., Li, Y.M., Imani, F., Wojciechowicz, D., Yang, Z., Liu, F.T., Cerami, A., 1995. Identification of galectin-3 as a high-affinity binding protein for advanced glycation end products (AGE): a new member of the AGE-receptor complex [Article]. Molecular medicine (Cambridge, Mass.) 1 (6), 634–646. https://doi.org/10.1007/bf03401604.
Wang, F., Li, Y.M., Li, R.Y., Yang, Y.E., Wei, M., Ha, C., 2023. U0126 and BAY11-7082 Inhibit the Progression of Endometriosis in a Rat Model by Suppressing the MEK/ERK/NF-κB Pathway. Womens Health Rep (New Rochelle) 4 (1), 65–77. https://doi.org/10.1089/whr.2021.0151.
Weigert, J., Neumeier, M., Wanninger, J., Bauer, S., Farkas, S., Scherer, M.N., Schnitzbauer, A., Schäffler, A., Aslanidis, C., Schölmerich, J.r., Buechler, C., 2010. Serum Galectin-3 Is Elevated in Obesity and Negatively Correlates with Glycosylated Hemoglobin in Type 2 Diabetes. The Journal of Clinical Endocrinology & Metabolism 95 (3), 1404–1411. https://doi.org/10.1210/jc.2009-1619.
Woo, S.L., Xu, H., Li, H., Zhao, Y., Hu, X., Zhao, J., Guo, X., Guo, T., Botchlett, R., Qi, T., Pei, Y., Zheng, J., Xu, Y., An, X., Chen, L., Chen, L., Li, Q., Xiao, X., Huo, Y., Wu, C., 2014. Metformin ameliorates hepatic steatosis and inflammation without altering adipose phenotype in diet-induced obesity. PLoS One 9 (3), e91111. https://doi.org/10.1371/journal.pone.0091111.
Wu, M., Xu, H., Liu, J., Tan, X., Wan, S., Guo, M., Long, Y., Xu, Y., 2021. Metformin and Fibrosis: A Review of Existing Evidence and Mechanisms. J Diabetes Res 2021, 6673525. https://doi.org/10.1155/2021/6673525.
Yamashita, S., Hashimoto, K., Sawada, I., Ogawa, M., Nakatsuka, E., Kawano, M., Kinose, Y., Kodama, M., Sawada, K., Kimura, T., 2022. Endometrial galectin-3 causes endometriosis by supporting eutopic endometrial cell survival and engraftment in the peritoneal cavity. American Journal of Reproductive Immunology 87 (6), e13533. https://doi.org/10.1111/aji.13533.

Yilmaz, B., Sucak, A., Kilic, S., Aksakal, O., Aksoy, Y., Lortlar, N., Sut, N., Gungor, T., 2010. Metformin regresses endometriotic implants in rats by improving implant levels of superoxide dismutase, vascular endothelial growth factor, tissue inhibitor of metalloproteinase-2, and matrix metalloproteinase-9. Am J Obstet Gynecol 202 (4). https://doi.org/10.1016/j.ajog.2009.10.873 368.e361-368.

Zhang, J., Xu, H., Zhou, X., Li, Y., Liu, T., Yin, X., Zhang, B., 2017. Role of metformin in inhibiting estrogen-induced proliferation and regulating ERα and ERβ expression in human endometrial cancer cells. Oncol Lett 14 (4), 4949–4956. https://doi.org/10.3892/ol.2017.6877.

Zhang, X., Zhang, C., Shen, S., Xia, Y.j., Yi, L., Gao, Q., Wang, Y., 2013. Dehydroepiandrosterone induces ovarian and uterine hyperfibrosis in female rats. Human Reproduction 28 (11), 3074–3085. https://doi.org/10.1093/humrep/det341.

Zhang, Y., Liu, Y., Liu, X., Yuan, X., Xiang, M., Liu, J., Zhang, L., Zhu, S., Lu, J., Tang, Q., Cheng, S., 2022. Exercise and Metformin Intervention Prevents Lipotoxicity-Induced Hepatocyte Apoptosis by Alleviating Oxidative and ER Stress and Activating the AMPK/Nrf2/HO-1 Signaling Pathway in db/db Mice. Oxidative Medicine and Cellular Longevity 2022, 2297268. https://doi.org/10.1155/2022/2297268.

Received 16 May 2024; received in revised form 20 September 2024; accepted 25 September 2024.